# Mysterious effects of olfactory pathway lesions on intestinal immunodeficiency targeting Peyer's patches: The first experimental study

Binali Firinci[a], Ozgur Caglar[a], Erdem Karadeniz[b], Ali Ahiskalioglu[c], Tuba Demirci[d], Mehmet Dumlu Aydin[e],*

[a] Ataturk University, Medical Faculty, Department of Pediatric Surgery, Erzurum, Turkey
[b] Ataturk University, Medical Faculty, Department of General Surgery, Erzurum, Turkey
[c] Ataturk University, Medical Faculty, Department of Anesthesiology and Reanimation, Erzurum, Turkey
[d] Ataturk University, Medical Faculty, Department of Histology, Erzurum, Turkey
[e] Ataturk University, Medical Faculty, Department of Neurosurgery, Erzurum, Turkey

## ARTICLE INFO

## ABSTRACT

*Background:* Although olfaction has been considered as important neuroimmunomodulatory foundation, there is no satisfying analytical information between neurohistomorphological features olfactory networks and intestinal immune system hardwares. We studied if the olfactory bulb lesions (OBL) may rely on histopathological features of intestinal lymphatic Peyer's patches in an animal model.
*Methods:* Thirty-two rats were grouped as control (Group I, n = 8), SHAM (Group II, n = 7) and OBL (Group III, n = 17) respectively; and followed eight weeks and animals were decapitated. The olfactory bulbs and intestines were extracted. Specimens stained with hematoxylin/eosin and GFAP methods and analyzed Stereologically to evaluate volume loss of olfactory bulbs and Peyer's patches volumes (PV) of intestines per cubic millimeter and compared with each other's statistically.
*Results:* The mean olfactory bulbs volumes were estimated as $3.65 \pm 0.32/mm^3$ in group I, $3.12 \pm 0.20/mm^3$ in group II and $2.21 \pm 0.15/mm^3$ in group III ($p < 0.0005$ Group III vs. I and II). The mean of PV were estimated as; $(9 \pm 2) \times 10^6\,\mu m^3/cm^3$ in Group-I, $(12 \pm 3) \times 10^6\,\mu m^3/cm^3$ in Group-II; and $(23 \pm 4) \times 10^6\,\mu m^3/cm^3$ in group-III ($p < 0.005$ Group II vs. I, $p < 0.0005$ Group III vs. I–II).
*Conclusions:* OBL could rely on intestinal immunodeficiency causing by olfaction loss induced denervation injury of Peyer's patches.

## Introduction

Intestinal immune functions are regulated by autonomic nervous system represented by the sympathetic splanchnic nerves, the parasympathetic S2–4 roots and especially vagus nerve in women [1]. The mucosal surface is the first barrier to pathogens [2]. Intestinal immunization are augmented by the olfactory informations [3]. Neuroenteric disorders seen in frequently in vagal insufficiency, but mostly ignored in clinical practice. Vagal nerve innervate small intestines and only proximal parts of bowels in man; and, all abdominopelvic organs in women [4]. Myenteric ganglia modulate the parasympathetic innervation by the vagal and sacral roots S2–S4. Interestingly, urogenital organs of womens are also innervated by vagal nerves, not men. Peyer's patches located on the mucosal surfaces and maintain intestinal immunity. Lymphoid tissue are more abundant in the lamina propria and

submucosa of the ileocecal orifice [5]. The Peyer's patches are mainly found in the jejunum and in the terminal ileum. Macrophages are common in the germinal centres of Peyer's patches [6]. Lymph nodes and Peyer's patches play in humoral and cell-mediated immune functions [7]. Phagocytes such as dendritic cells play a crucial role intestinal immunity [8]. Olfactory impulses mediate general immunity [9]. Dopaminergic inputs of olfactory nerves are essential for the intestinal immunity. Decreased sense of smell and taste reduce immune power of the intestines [10]. Vagal/sacral parasympathetic deverpation may cause intestinal immunodeficiency [11]. Vagal nerves innervate faringeal and intestinal lymph nodes [12]. Caudal lumbosacral (L6-S1) roots have parasympathetic and caudal thoracicrostral lumbar (T13-L1) spinal segments have sympathetics fibers that innervate gut, intestines and urogenital organs [13]. The sacral parasympathetic outflow to the large intestines come from Onuf's nucleus [14]. The Meissner's network

---

consists of small ganglia associated with the vascular submucosal plexus [15]. Although olfactory network stimulation induced vagal and sacral parasympathetics has been responsible for intestinal immunity, neither olfactory nerves nor its functions enoughly mentioned in the literature. In this study, it is examined if there is any relation between olfactory bulb lesion and denervation injury of intestinal Peyer's patches.

### Hypothesis

Olfaction have a potential role on immunity. Olfaction loss affect especially Peyer's patches. Olfaction loss causes intestinal immun failure. Although it is well known that there is a strong link between olfaction-vagal network-intestinal complexes there is no information what is the essential role of neural complex on immunological events. We hypothesized that olfactory informations play essential role on the development of intestinal immunity via vagal network. Because olfaction provide a wireless communication between external milieu and animal body. Olfactory impulses have potent affect on vagal network; and, vagal nerve is an important neuromodulator on the intestinal immunity.

### Materials and methods

The study protocol and permissions were reviewed and approved by the Ethics Committee for Animal Experiments, Faculty of Medicine, Ataturk University. The animals were managed and the experiments conducted according to the guidelines prescribed by the Committee.

This study was conducted on 32 (n = 32) rats, with 8 rats (n = 8) in the control group, 7 rats (n = 7) in the sham group, and 17 rats (n = 17) in the OBL group. The animals were divided to three groups. A balanced, injectable anesthetics was preferred to reduce pain. Anesthesia induced by isoflurane 0.2 mL/kg with subcutaneous (Ketamine HCL, 150 mg/1.5 mL; Xylazine HCL, 30 mg/1.5 mL; and distilled water, 1 mL). Frontal bone was shaved and an interpupillar midline burr hole was done. In GII, only burr hole was done and OBL not applied; but, bilaterally OBL was done in Group III. All animals observed eight weeks. Olfactory functions, appetite status and weights of animals were reported. After eight week, animals were decapitaded under general anesthesia. Tissues of all animals were stored in 10% formalin solutions for seven days and then embedded in liquid paraffin. Both the olfactory bulbs and intestinal sections were stained with haematoxylin-eosin and GFAP method were used for histological examination. Peyer's patches volumes per cubic centimeter and olfactory bulb volume values compared with statistically.

### Histopathological procedures

The intestines sectioned 5 μm at the distances of 30 μm. Every 30th and 31st sections were sampled for PV calculation. The total numbers of Peyer's patches studied by the fractionator method [16,17]. Each tissue sections were put on glass-slides and stained with haematoxylin-eosin (H&E), and GFAP method and examined with light microscope. The photographs were taken of the different growth between $40\times$ and $20\times$ magnifications. Brain materials were also stained with same methods. The following procedures were done as same as the Karadeniz et al. methods [18].

### Stereological analysis

Stereology has become the most efficient method [19] that provide simple and reliable parameters, such as the total volume, number and size of cells or particles. We used paired-sampled sections choosen by randomly a starting point within the first 30-section interval and every neighbor of 30th section were sampled. The sampling fraction sections

(f1) were fused with another sections and proportional values estimated with f1 = 1/30 formula. We decided to use physical dissector method to evaluate the numbers of Peyer's patches. The dissector pairs named as eference and look-up sections to calculate double number of dissector pairs without taking new sections. The number of calculated Peyer's patches was designated $\Sigma Q^-$. The total numbers of Peyer's patches (N), in intestines were calculated from the equation $N = \Sigma Q^- \times 1/f1 \times 1/f2$. Kolmogorov-Smirnov and Shapiro-Wilk methods used to test our parameters ($p < 0.05$). Before scoring of datas, Mann-Whitney-*U* test was applied for the groups, and then analyzed with Kruskal-Wallis test. The p values were thought statistically significant for $\leq 0.0098$). The p value was accepted significant at the level of 0.05 (Confidence interval 95%).

After calculating procedure, Total PV (TPV) was estimated via summation of each PV volumes. Peyer's patches was thought as a ellipsoid shape, and the a, b, and c are half of the ellipsoid axis in x, y, and z apsis and their volumes was calculated at the following formula:

$$\sum_1^n TPV = \sum_{f=1}^n n [\![\frac{4}{3}\pi \left\langle \frac{a+b+c}{3} \right\rangle^3 ]\!]^*$$

The physical dissector method was preferred to evaluate the numbers of Peyer's patches. The mean numerical density of the Peyer's patches per/cm$^3$ intestinal tissue (Nt/Gt) per/mm$^3$ was calculated using the following formula that used for breast tissue in our former study by Karadeniz et al. [18].

$$\frac{Nt}{Gt} = \frac{\sum Q^-}{\sum A}/xd$$

where $\Sigma Q^-$N is the total number of Peyer's patch existing only in the reference sections, d is the section thickness, and A is the area of the counting frame. The most useful method to calculate of $\Sigma A$ is: $\Sigma A = \Sigma Pa. \Sigma P$. The Cavalieri used to obtain the total number of Peyer's patches. The total number of Peyer's patches calculated by multiplication of the volume (mm$^3$) and the numerical density of Peyer's patches. The differences between the TPV and olfactory bulb volume values were compared statistically by software package (SPSS® for Windows v. 12.0, Chicago, USA). The data analysis consisted of the Kruskal-Wallis and Mann-Whitney *U* test. Differences were accepted to be significant at $p < 0.05$.

### Results

Neck stiffness, unconsciousness, convulsive attacks, fever, apnea, cardiac arrhythmia, and breathing disturbances were reported in study group especially dead animals (n = 3).

### Histopathological Results

Fig. 1 show olfactory bulb and small intestines with Peyer's patches. Small intestines with Peyer's patches and volume value estimation formula is seen in GI in Fig. 2. Fig. 3 shows small intestine with Peyer's patches and total volume value estimation formula is seen by a cubic centimeter. In Fig. 4, partially swollen Peyer's patches are seen in GII. Swollen Peyer's patches and destructed intestinal structures in GIII (Fig. 5). Histological appearances of normal intestines with myenteric plexuses with swollen Peyer's patches and destructed intestinal structures are seen in GIII (Fig. 6).

### Numerical results

Anosmia and memory loss were observed in OBL applied animals. The mean olfactory bulbs volumes were estimated as $3.65 \pm 0.32$/mm$^3$ in group I, $3.12 \pm 0.20$/mm$^3$ in group II and $2.21 \pm 0.15$/mm$^3$ in group III ($p < 0.0005$ Group III vs. I and II). The mean of PV were
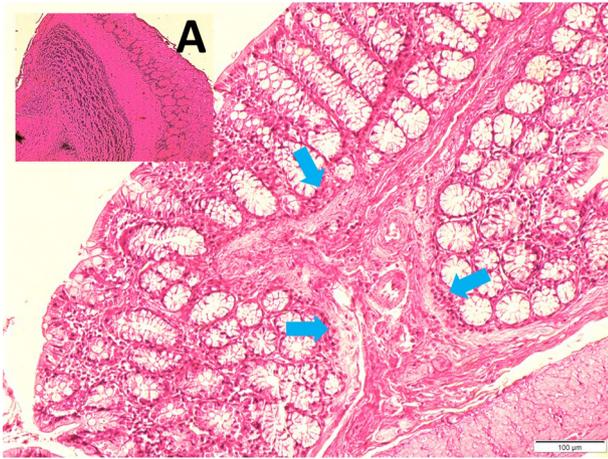
**Fig. 1.** Olfactory bulb (LM,H&E,x4/A) and small intestine with Peyer's patches (Arrows) are seen (LM,H&E,x10/Base).



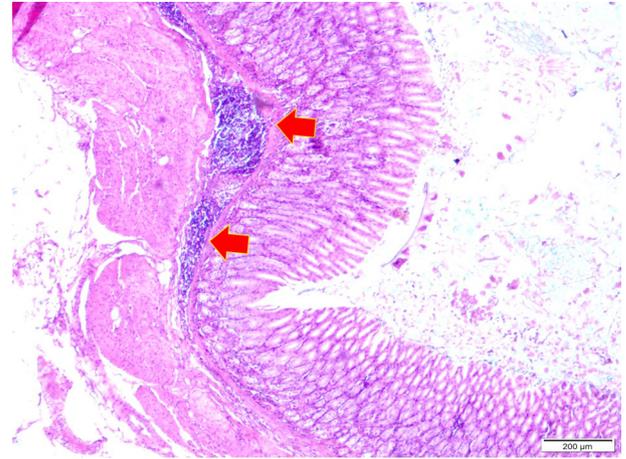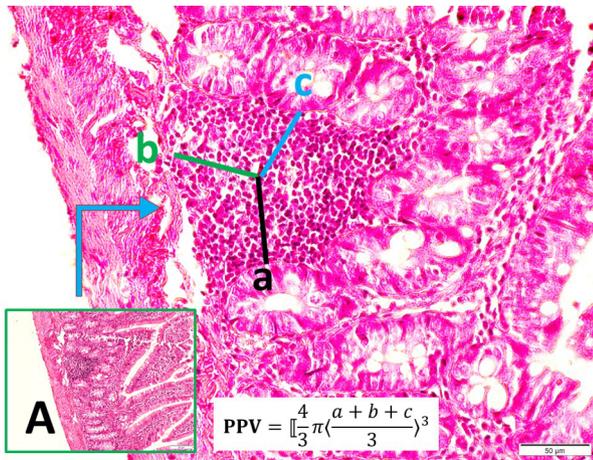**Fig. 2.** Small intestine with Peyer's patches (LM,H&E,x10/A), magnified form (LM,H&E,x20) and volume value estimation formula is seen in a normal animal.
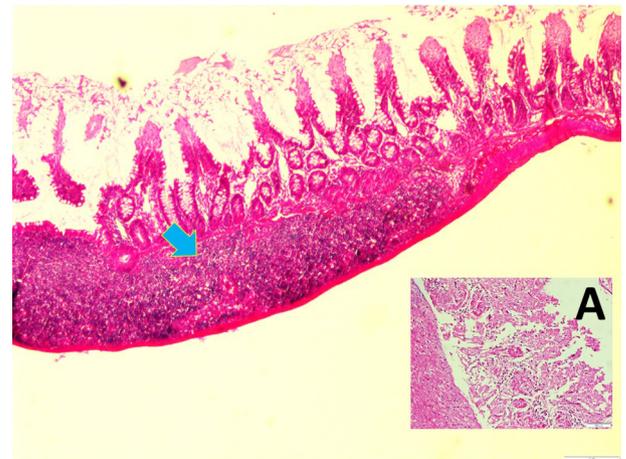
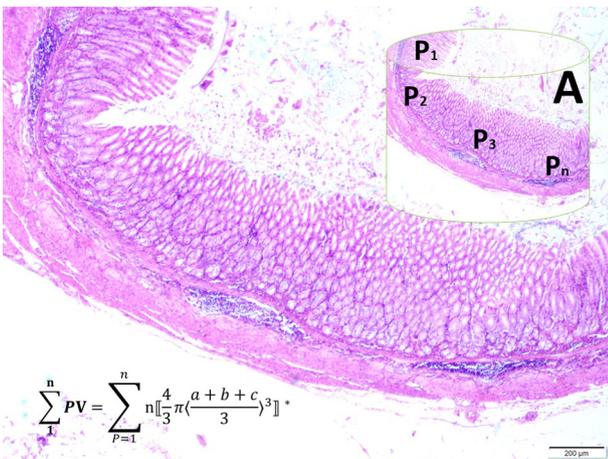$$PPV = \llbracket \frac{4}{3}\pi\langle\frac{a+b+c}{3}\rangle^3$$



**Fig. 3.** Small intestine with Peyer's patches (Arrows) (LM,H&E,x10/A) and total volume value estimation formula is seen by a cubic centimeter (A).

$$\sum_{1}^{n} PV = \sum_{P=1}^{n} n\llbracket\frac{4}{3}\pi\langle\frac{a+b+c}{3}\rangle^3\rrbracket^*$$



**Fig. 4.** Partially swollen Peyer's patches is seen in a SHAM group (LM,H&E, x4).



**Fig. 5.** Swollen Peyer's patches (Arrow) and destructed intestinal structures (LM,H&E,x4/Base) in a OBL (LM,H&E,x10/A) applied animal.
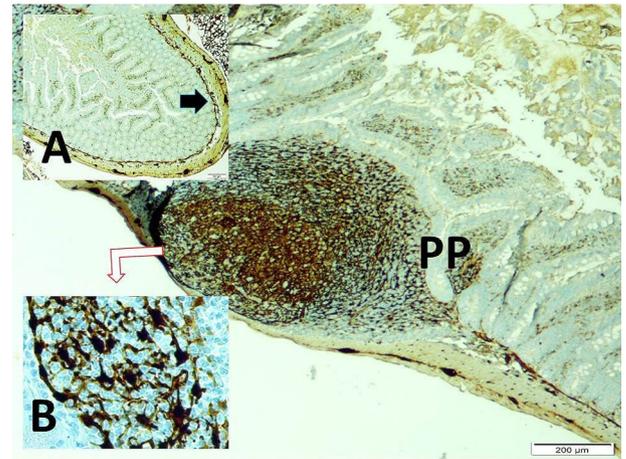


**Fig. 6.** Normal intestine with myenteric plexuses (LM,GFAP,x10/A) wollen Peyer's patches (Arrow) and destructed intestinal structures (LM,NSE,x4/Base) in a OBL (LM,H&E,x10/A) applied animal.

estimated as; $(9 \pm 2) \times 106\,\mu m^3/cm^3$ in Group-I, $(12 \pm 3) \times 106\,\mu m^3/cm^3$ in Group-II; and $(23 \pm 4) \times 106\,\mu m^3/cm^3$ in group-III ($p < 0.005$ Group II vs. I, $p < 0.0005$ Group III vs. I-II). Results were summarised in table 1.

## Discussion

Intestinal immunity is regulated by Peyer's patches innervated by myenteric ganglia managed with vagal and sacral parasympathetic networks. Intestinal immunization are augmented by the conscious/

**Table 1**
Numerical results of study.

|  | Group I | Group II | Group III |
|---|---|---|---|
| Olfactory bulb volume (mm$^3$) | 3.65 ± 0.32 | 3.12 ± 0.20 | 2.21 ± 0.15$^\alpha$ |
| Peyer's Patches volume (×10$^6$ μm$^3$/cm$^3$) | 9 ± 2 | 12 ± 3$^\beta$ | 23 ± 4$^\alpha$ |

The values represent the mean ± standard deviation, Group I: Control Group (n = 8), Group II (n = 7): SHAM group, Group III (n = 17): study group.

$^\alpha$ $p < 0.0005$ Group III vs. I–II.
$^\beta$ $p < 0.005$ Group II vs. I.

unconscious stimulations of olfactory nerves [3].

*Histology of Peyer's patches*

Lymph nodes and Peyer's patches play in humoral and cell-mediated immune functions of intestines [7]. Peyer's patches frequently located submucosal surfaces of the cecum and the 1/3 of the colon. Whereas, lymphoid tissues are located under lamina propria and submucosal regions. The mucosa-associated lymphoid tissues consist of higher number of lymphoid follicles than that of the larger bowel [5]. Each patch is formed by many elongated dome regions flanked by intestinal villi in villi. The lymphoid follicles express clear germinal centers [20]. Macrophages are common in the germinal centres. Caecal Peyer's patches consists of numerous secondary follicles in the lamina propria [6]. Compartmentalization of primary lymphoid follicles started about 14 days after birth and secondary follicles are seen from about 18 days and matured at about 4 weeks after birth. Peripartum nutrition is crucial for developing the immune system of neonates [21]. Dendritic cells, macrophages and B-cells cells of intestines [22] secrete various immunoglobulins [23]. T-lymphocytes predominant among the lymphoid cells [24]. Peyer's patch shows unusual vessels in granulomas of the immature Peyer's patch [25].

Peyer's patches located in the small intestine [26]. The Peyer's patches plays an essential role as a barrier of the gastrointestinal immunity [27]. This mucus layer not only prevents inflammation but also plays an essential role in microbiota colonization [28]. Phagocytes such as dendritic cells and macrophages play a crucial role in maintaining intestinal immunity [8]. Immunoglobulin A induce primary stimulus of intestinal Peyer's patches [29]. Dendritic cells play a central role in immune responses of intestines [30].

Peyer's patches are immune sensors in intestines [31]. The distribution, size, and appearance of Peyer's patches vary according to species. Peyer's patches are nodules that play a central role in intestinal immunity [32]. Immune responses against to the enteric microflora may change olfactory nerve impulses [33]. Intra-uterine growth restriction effect on Peyer's patches maturity [34]. Ischemic stroke significantly damage intestinal immunity [35].

*Myenteric plexus and intestinal relations*

The plexus of Meissner have a closely relation to the external surface of intestines [14] and located in submucosa and smooth muscle cells [14]. Meissner's plexus consists of the more small ganglia under submucosal plexus, Peyer's patches, blood vessels of intestines. The majority of the lymphoid organs are richly innervated by submucosal plexus. Auerbach plexus is a network as small meshes of intestines and stimulate Peyer's patches [36]. At the presented study, it was shown that myenteric network is innervated by Onuf's nucleus centralized S2-4 nerve roots; and any lesion of that network may induce Hirschsprung/Ogilvie mimicking pathologies and intestinal immunodeficiency.

*Nerves of Peyer's patches*

Innervation Peyer's patch have important roles on intestinal immunity. Peyer's patches are innervated various autonomic nerves such as vagus, Onuf nucleus centralized sacral parasympathetics, myenteric plexus and sympathetics [37]. Trigeminal and vagal nerves innervate faringeal and intestinal lymph nodes [12]. Peyer's patches are the first colonization sites for infectious prions. Dendritic cells include valuable antigen-producing cells opposed to some nerves and formed membrane-membrane contact with synaptic clefts [38]. Lymphoid nodules in the Peyer's patches make important networks among nerve fibres, follicular dendritic cells and macrophages [39]. Dopaminergic nerve endings are observed in the fibers around and within Peyer's patches, trigeminal, glossopharyngeal, vagal, sympathetic ganglia [40]. Prion protein accumulation [41] firstly seen in the enteric ganglia [42] such as Peyer's patches, lymphoid centers, Meissner's and Auerbach's networks, solar trunk and spinal ganglia [43].

*Inflammation of Peyer's patches*

The mucosal surface of the intestine is the first barrier to pathogens [2]. Gastrointestinal microbiota may influence local and systemic inflammation [44]. In the small intestine, Peyer's patches are the most important of these mucosal immune response inductive sites [45] with their T follicular helper cells in Peyer's patches promote high-affinity IgA responses [46]. Visceral lymph node drains adipose tissue and exacerbate systemic pro-inflammation. Visceral lymph nodes plays a fundamental role in exacerbation of systemic pro-inflammation in obese persons [47]. Lymphoid organ hypertrophy is a hallmark of localized infection [15]. Salmonella and non-pathogenic E. coli cause intestinal Peyer's patches inflammation [48].

The response of dendritic cells in Peyer's patches within the first 48 h of infection is very useful [49]. Crohn's disease, ulcerative colitis is an inflammatory processes that result from nervous insufficiency [50]. Recurrent Crohn's disease cause inflammatory process in Peyer's patches [51]. Toxic microparticles accumulate in cells of Peyer's patches [52]. Salmonella localized in jejunal Peyer's patch mucosa in immunodeficiency persons [53]. Escherichia coli infections associate Crohn's disease and Peyer's patches [54]. Brucella melitensis [55] and Escherichia coli [56] domed villi of jejunal-ileal Peyer's patches [57].

*Hyperplasia of Peyer's patches*

Mucosa-associated lymphomas usually arise at sites of Peyer's patches [58]. Rotaviruses cause lymphoid hypertrophy and hyperplasia of Peyer's patches [59]. Brucella abortus and the germinal center response in draining brachial lymph nodes located around Peyer's patches [60]. Common variable immunodeficiency with hypogammaglobulinemia is often complicated by nodular lymphoid hyperplasia of the intestine [61] Giardia muris were surrounded by rosettes of lymphoblasts in the epithelium deficient in lymphocytes into Peyer's patch lymphoid follicles [62].

*Olfaction and intestinal immunological functions*

Olfactory impulses are a wireless communication web between animals and the environment. Olfactory bulb stimulate the other brain centers to start neuroimmunological activity. Olfactory dysfunctions appears at early stages of neuropsychiatric disease and neuroautoimmune conditions [63]. HIV infection is frequently seen in olfaction deficient patients [64]. Intestinal immunodeficiency are frequently seen in neurodegenerative disease associated with olfaction disorders [65]. Psychiatric diseases are often associated with mild alterations in immune functions together with olfaction disorders [66]. Smell lose has been considered a less important sense for neuroimmunity and neurodegenerative-neuropsychiatric-collagen tissue diseases [67]. Decreased sense of smell and taste cause decreased intestinal metabolism [10]. The piriform cortex has been the focus of the regulation of intestinal functions [68]. Mucosal immunity are augmented by the olfactory

impulses [3]. Olfactory impulses regulate intestinal immunologic functions [9]. Dopaminergic impulses of olfactory bulbs reach to substantia nigra, ventral tegmental area and manage gastronteric immune functions. For decreased intestinal immunity develops such as Parkinson's disease, schizophrenia and depression [69]. Olfaction disorders could cause depression [70], mammary gland degeneration [18] and hypothyroidism [17] that these pathological problems should be accepted as an important causes of neuroimmunolgical and intestinal immunological deficiencies which has not been extensively studied so far.

*Olfaction and microbiata*

If olfaction disorders could cause intestinal immunodeficiency and peyer's patches degeneration, easily hypothesized that olfaction disorders may affect intestinal microbiota species and floral changes. This situation may have major clinical importance. For example, the intestinal microbiota affects all physiologic, endocrine, immunologic, metabolic functions and social interactions [71]. Some neurodegenerative disorders such as Parkinson's disease [72], inflammatory bowel disease [73] could be attributed to microbiota changes. Interestingly the microbiota-gut-brain axis line explains why alterations in microbiota alters nervous system functions and pathological behaviors such as autism [74] and obsessive-compulsive disorders [75]. Intestinal microbiota may change blood-brain barrier and cerebrospinal fluid content [76].

## Conclusion

Although there is a wide relations between olfactory impulses and body immunity, it is very interesting that there is no enough information. Also, olfactory impulses are necessary for the nutrition and propagation requiring behaviours regulated by especially autonomic and and some voluntary nervous system. The effect of olfactory network softwares has been thoroughly observed and produced knowledges have been used extensively by humankind; but, their immunological effects have not been observed in required as well as deserved. It seems that OBL related anosmia may be responsible for general or intestinal immunodeficiency because OBL may cause in both immunodeficiency resembling clinical and also neuropathological findings in PV OBL animals which has not been mentioned in the literature. This issue needs new investigations and new insights in the future.

## Funding statement

## Conflicts of interest

The authors declare no competing interests.

## Appendix A. Supplementary data

Supplementary data to this article can be found online at https://doi.org/10.1016/j.mehy.2019.02.032.

## References:

[1] He JH, Wang Q, Cai QP, et al. Quantitative anatomical study of male pelvic autonomic plexus and its clinical potential in rectal resection. Surg Radiol Anat 2010;32:783–90.

[2] Reis BS, Mucida D. The role of the intestinal context in the generation of tolerance and inflammation. Clin Dev Immunol 2012;2012:157948.

[3] Fujihashi K, Kato H, van Ginkel FW, et al. A revisit of mucosal IgA immunity and oral tolerance. Acta Odontol Scand 2001;59:301–8.

[4] Eaker EY, Bixler GB, Dunn AJ, Moreshead WV, Mathias JR. Chronic alterations in jejunal myoelectric activity in rats due to MPTP. Am J Physiol 1987;253:G809–15.

[5] ZhaXi Y, Wang W, Zhang W, Gao Q, Guo M, Jia S. Morphologic observation of mucosa-associated lymphoid tissue in the large intestine of Bactrian camels (Camelus bactrianus). Anat Rec (Hoboken, N.J.: 2007) 2007;297:1292–301.

[6] Connolly JH, Canfield PJ, McClure SJ, Whittington RJ. Histological and immunohistological investigation of lymphoid tissue in the platypus (Ornithorhynchus anatinus). J Anat 1999;195(Pt 2):161–71.

[7] Koike R, Nishimura T, Yasumizu R, et al. The splenic marginal zone is absent in alymphoplastic aly mutant mice. Eur J Immunol 1996;26:669–75.

[8] Morikawa M, Tsujibe S, Kiyoshima-Shibata J, et al. Microbiota of the small intestine is selectively engulfed by phagocytes of the lamina propria and Peyer's patches. PLoS One 2016;11:e0163607.

[9] Oh U, Jung J. Cellular functions of TMEM16/anoctamin. Pflugers Arch 2016;468:443–53.

[10] Norin E. Intestinal cholesterol conversion in adults and elderly from four different European countries. Ann Nutr Metab 2008;52(Suppl. 1):12–4.

[11] Sakakibara R, Odaka T, Uchiyama T, et al. Colonic transit time and rectoanal videomanometry in Parkinson's disease. J Neurol Neurosurg Psychiatry 2003;74:268–72.

[12] Kimura S, Muto M, Hisamoto M, Zheng M, Iwanaga T. A novel type of cells expressing GP2 in the respiratory epithelium of the paranasal sinuses in mice. Biomed Res (Tokyo, Japan) 2014;35:329–37.

[13] Vizzard MA, Brisson M, de Groat WC. Transneuronal labeling of neurons in the adult rat central nervous system following inoculation of pseudorabies virus into the colon. Cell Tissue Res 2000;299:9–26.

[14] Scheuermann DW, Stach W, Timmermans JP. Topography, architecture and structure of the plexus submucosus internus (Meissner) of the porcine small intestine in scanning electron microscopy. Acta Anat 1987;129:96–104.

[15] Schulz O, Ugur M, Friedrichsen M, et al. Hypertrophy of infected Peyer's patches arises from global, interferon-receptor, and CD69-independent shutdown of lymphocyte egress. Mucosal Immunol 2014;7:892–904.

[16] Aydin MD, Kanat A, Turkmenoglu ON, Yolas C, Gundogdu C, Aydin N. Changes in number of water-filled vesicles of choroid plexus in early and late phase of experimental rabbit subarachnoid hemorrhage model: the role of petrous ganglion of glossopharyngeal nerve. Acta Neurochir (Wien) 2014;156:1311–7.

[17] Aydin N, Ramazanoglu L, Onen MR, et al. Rationalization of the irrational neuropathologic basis of hypothyroidism-olfaction disorders paradox: experimental study. World Neurosurg 2017;107:400–8.

[18] Karadeniz E, Kocak MN, Ahiskalioglu A, et al. Exploring of the unpredicted effects of olfactory network injuries on mammary gland degeneration: a preliminary experimental study. J Invest Surg 2018:1–8.

[19] Kanat A. Pathophysiology of acute hydrocephalus after subarachnoid hemorrhage. World Neurosurg 2014;82:e386–7.

[20] Zidan M, Pabst R. Unique microanatomy of ileal peyer's patches of the one humped camel (Camelus dromedarius) is not age-dependent. Anat Rec (Hoboken, N.J.: 2007) 2007;291:1023–8.

[21] Le Bourgot C, Ferret-Bernard S, Le Normand L, et al. Maternal short-chain fructooligosaccharide supplementation influences intestinal immune system maturation in piglets. PLoS One 2014;9:e107508.

[22] Mann ER, Li X. Intestinal antigen-presenting cells in mucosal immune homeostasis: crosstalk between dendritic cells, macrophages and B-cells. World J Gastroenterol 2014;20:9653–64.

[23] Sminia T, Janse EM, Plesch BE. Ontogeny of Peyer's patches of the rat. Anat Rec 1983;207:309–16.

[24] Chetvertnykh VA. Morphofunctional features of 10–12-day-old rabbit lymphoid tissue. Arkh Anat Gistol Embriol 1981;80:64–9.

[25] Nightingale G, Hurley JV. Relationship between lymphocyte emigration and vascular endothelium in chronic inflammation. Pathology 1978;10:27–44.

[26] Wagner C, Bonnardel J, Da Silva C, Martens L, Gorvel JP, Lelouard H. Some news from the unknown soldier, the Peyer's patch macrophage. Cell Immunol 2018.

[27] Qiu Z, Sheridan BS. Isolating lymphocytes from the mouse small intestinal immune system. J Visualized Exp JoVE 2018.

[28] Elderman M, Sovran B, Hugenholtz F, et al. The effect of age on the intestinal mucus thickness, microbiota composition and immunity in relation to sex in mice. PLoS One 2017;12:e0184274.

[29] Reboldi A, Arnon TI, Rodda LB, Atakilit A, Sheppard D, Cyster JG. IgA production requires B cell interaction with subepithelial dendritic cells in Peyer's patches. Science (New York, NY) 2016;352:aaf4822.

[30] Bekiaris V, Persson EK, Agace WW. Intestinal dendritic cells in the regulation of mucosal immunity. Immunol Rev 2014;260:86–101.

[31] Gao F, Li M, Liu Y, Gao C, Wen S, Tang L. Intestinal dysbacteriosis induces changes of T lymphocyte subpopulations in Peyer's patches of mice and orients the immune response towards humoral immunity. Gut Pathogens 2012;4:19.

[32] Fujimoto K, Fujii G, Sakurai H, Yoshitome H, Mutoh M, Wada M. Intestinal Peyer's patches prevent tumorigenesis in Apc (Min/+) mice. J Clin Biochem Nutr 2015;56:43–8.

[33] Hakansson A, Tormo-Badia N, Baridi A, et al. Immunological alteration and changes of gut microbiota after dextran sulfate sodium (DSS) administration in mice. Clin Exp Med 2015;15:107–20.

[34] Attig L, Brisard D, Larcher T, et al. Postnatal leptin promotes organ maturation and development in IUGR piglets. PLoS One 2013;8:e64616.

[35] Liu Y, Luo S, Kou L, et al. Ischemic stroke damages the intestinal mucosa and induces alteration of the intestinal lymphocytes and CCL19 mRNA in rats. Neurosci Lett 2017;658:165–70.

[36] Driessen A, Creemers J, Geboes K. The innervation of the lymphoid tissue at the ileocolonic transition: an enzyme and immunohistochemical study. Acta Anat

(Basel) 1992;144:304–10.

[37] Stead RH. Innervation of mucosal immune cells in the gastrointestinal tract. Reg Immunol 1992;4:91–9.

[38] Ma B, von Wasielewski R, Lindenmaier W, Dittmar KE. Immmunohistochemical study of the blood and lymphatic vasculature and the innervation of mouse gut and gut-associated lymphoid tissue. Anat Histol Embryol 2007;36:62–74.

[39] Heggebo R, Gonzalez L, Press CM, Gunnes G, Espenes A, Jeffrey M. Disease-associated PrP in the enteric nervous system of scrapie-affected Suffolk sheep. J Gen Virol 2003;84:1327–38.

[40] Russo D, Fantaguzzi CM, Di Guardo G, et al. Characterization of sheep (Ovis aries) palatine tonsil innervation. Neuroscience 2009;161:813–26.

[41] McGovern G, Martin S, Gonzalez L, Witz J, Jeffrey M. Frequency and distribution of nerves in scrapie-affected and unaffected Peyer's patches and lymph nodes. Vet Pathol 2009;46:233–40.

[42] van Keulen LJ, Vromans ME, Dolstra CH, Bossers A, van Zijderveld FG. Pathogenesis of bovine spongiform encephalopathy in sheep. Arch Virol 2008;153:445–53.

[43] Narita M, Kimura K, Tanimura N, Arai S, Uchimura A. Immunohistochemical demonstration of spread of Aujeszky's disease virus to the porcine central nervous system after intestinal inoculation. J Comp Pathol 1998;118:329–36.

[44] Stojanovska V, McQuade RM, Fraser S, et al. Oxaliplatin-induced changes in microbiota, TLR4+ cells and enhanced HMGB1 expression in the murine colon. PLoS One 2018;13:e0198359.

[45] Cordonnier C, Etienne-Mesmin L, Thevenot J, et al. Enterohemorrhagic Escherichia coli pathogenesis: role of long polar fimbriae in Peyer's patches interactions. Sci Rep 2017;7:44655.

[46] Proietti M, Cornacchione V, Rezzonico Jost T, et al. ATP-gated ionotropic P2X7 receptor controls follicular T helper cell numbers in Peyer's patches to promote host-microbiota mutualism. Immunity 2014;41:789–801.

[47] Shimokawa C, Senba M, Kobayashi S, et al. Intestinal inflammation-mediated clearance of amebic parasites is dependent on IFN-gamma. J Immunol (Baltimore Md) 1950;200(2018):1101–9.

[48] Willer Y, Muller B, Bumann D. Intestinal inflammation responds to microbial tissue load independent of pathogen/non-pathogen discrimination. PLoS One 2012;7:e35992.

[49] Lopez-Guerrero DV, Meza-Perez S, Ramirez-Pliego O, et al. Rotavirus infection activates dendritic cells from Peyer's patches in adult mice. J Virol 2010;84:1856–66.

[50] Koboziev I, Karlsson F, Grisham MB. Gut-associated lymphoid tissue, T cell trafficking, and chronic intestinal inflammation. Ann NY Acad Sci 2010;1207(Suppl. 1):E86–93.

[51] Salim SY, Silva MA, Keita AV, et al. CD83+CCR7− dendritic cells accumulate in the subepithelial dome and internalize translocated Escherichia coli HB101 in the Peyer's patches of ileal Crohn's disease. Am J Pathol 2009;174:82–90.

[52] Becker HM, Bertschinger MM, Rogler G. Microparticles and their impact on intestinal immunity. Dig Dis (Basel, Switzerland) 2012;30(Suppl. 3):47–54.

[53] Hyland KA, Brown DR, Murtaugh MP. Salmonella enterica serovar Choleraesuis infection of the porcine jejunal Peyer's patch rapidly induces IL-1beta and IL-8 expression. Vet Immunol Immunopathol 2006;109:1–11.

[54] Vazeille E, Chassaing B, Buisson A, et al. GipA factor supports colonization of Peyer's patches by Crohn's disease-associated Escherichia coli. Inflamm Bowel Dis 2016;22:68–81.

[55] Rossetti CA, Drake KL, Siddavatam P, et al. Systems biology analysis of Brucella infected Peyer's patch reveals rapid invasion with modest transient perturbations of the host transcriptome. PLoS One 2013;8:e81719.

[56] Pieper R, Zhang Q, Clark DJ, et al. Proteomic view of interactions of shiga toxin-producing Escherichia coli with the intestinal environment in gnotobiotic piglets.

[57] Heidegger S, Anz D, Stephan N, et al. Virus-associated activation of innate immunity induces rapid disruption of Peyer's patches in mice. Blood 2013;122:2591–9.

[58] Attygalle AD, Liu H, Shirali S, et al. Atypical marginal zone hyperplasia of mucosa-associated lymphoid tissue: a reactive condition of childhood showing immunoglobulin lambda light-chain restriction. Blood 2004;104:3343–8.

[59] Moser CA, Dolfi DV, Di Vietro ML, Heaton PA, Offit PA, Clark HF. Hypertrophy, hyperplasia, and infectious virus in gut-associated lymphoid tissue of mice after oral inoculation with simian-human or bovine-human reassortant rotaviruses. J Infect Dis 2001;183:1108–11.

[60] Secord EA, Edington JM, Thorbecke GJ. The Emu-bcl-2 transgene enhances antigen-induced germinal center formation in both BALB/c and SJL mice but causes age-dependent germinal center hyperplasia only in the lymphoma-prone SJL strain. Am J Pathol 1995;147:422–33.

[61] Van den Brande P, Geboes K, Vantrappen G, et al. Intestinal nodular lymphoid hyperplasia in patients with common variable immunodeficiency: local accumulation of B and CD8(+) lymphocytes. J Clin Immunol 1988;8:296–306.

[62] Owen RL, Allen CL, Stevens DP. Phagocytosis of Giardia muris by macrophages in Peyer's patch epithelium in mice. Infect Immun 1981;33:591–601.

[63] Strous RD, Shoenfeld Y. To smell the immune system: olfaction, autoimmunity and brain involvement. Autoimmun Rev 2006;6:54–60.

[64] Zucco GM, Ingegneri G. Olfactory deficits in HIV-infected patients with and without AIDS dementia complex. Physiol Behav 2004;80:669–74.

[65] De Virgilio A, Greco A, Fabbrini G, et al. Parkinson's disease: autoimmunity and neuroinflammation. Autoimmun Rev 2016;15:1005–11.

[66] Ortega-Hernandez OD, Kivity S, Shoenfeld Y. Olfaction, psychiatric disorders and autoimmunity: is there a common genetic association? Autoimmunity 2009;42:80–8.

[67] Moscavitch SD, Szyper-Kravitz M, Shoenfeld Y. Autoimmune pathology accounts for common manifestations in a wide range of neuro-psychiatric disorders: the olfactory and immune system interrelationship. Clin Immunol (Orlando, Fla) 2009;130:235–43.

[68] Ekstrand JJ, Domroese ME, Johnson DM, et al. A new subdivision of anterior piriform cortex and associated deep nucleus with novel features of interest for olfaction and epilepsy. J Comp Neurol 2001;434:289–307.

[69] Michael AC, Borland L. Electrochemical methods for neuroscience. CRC Press; 2006.

[70] Oral E, Aydin MD, Aydin N, et al. How olfaction disorders can cause depression? The role of habenular degeneration. Neuroscience 2013;240:63–9.

[71] Wong AC, Wang QP, Morimoto J, et al. Gut microbiota modifies olfactory-guided microbial preferences and foraging decisions in drosophila. Curr Biol 2017;27. p. 2397–404 e2394.

[72] Berstad K, Berstad JER. Parkinson's disease; the hibernating spore hypothesis. Med Hypotheses 2017;104:48–53.

[73] Liptak R, Gromova B, Maronek M, Gardlik R. Reverse phenotype transfer via fecal microbial transplantation in inflammatory bowel disease. Med Hypotheses 2019;122:41–4.

[74] Weston B, Fogal B, Cook D, Dhurjati P. An agent-based modeling framework for evaluating hypotheses on risks for developing autism: effects of the gut microbial environment. Med Hypotheses 2015;84:395–401.

[75] Rees JC. Obsessive-compulsive disorder and gut microbiota dysregulation. Med Hypotheses 2014;82:163–6.

[76] Kazakos EI, Kountouras J, Polyzos SA, Deretzi G. Novel aspects of defensins' involvement in virus-induced autoimmunity in the central nervous system. Med Hypotheses 2017;102:33–6.